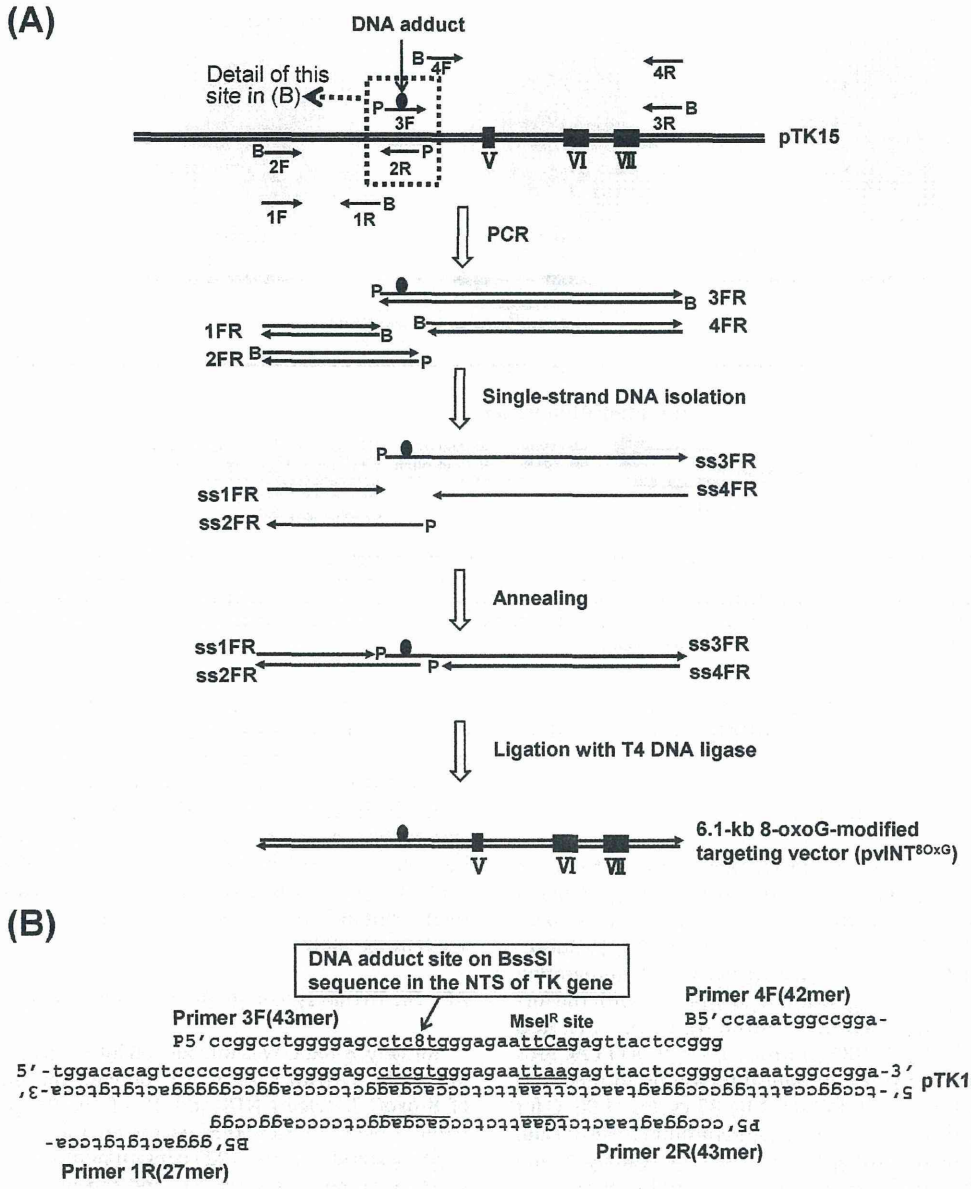

Fig. 2. PCR-based construction of a targeting vector containing a single 8-oxoG. (A) Diagram of pvINT^{8OxG} vector preparation; The P and B at the 5′-terminus of the oligodeoxynucleotides indicate phosphorylation and biotinylation, respectively. (B) Details of the site of 8-oxoG modification; the adduct is indicated by "8" in Primer 3F. We inserted 8-oxoG in place of the central guanine at the *Bss*SI site in *TK*-NTS (5′-CTCGTG in Primer 3F) to generate the pvINT^{8OxG} vector. The *MseI*^{R} site was also placed near the site in the 3F and 2R primers.

mutation in exon 4 on the other *TK* allele. An I-*Sce*I site exists on the original exon 5 region (Fig. 3A), which allows generation of wild-type *TK* by correct targeting using pvINT^{8OxG} or pvINT^{G} vectors. Subsequently, *TK* revertant clones (*TK*+/−) can be selected using HAT (Fig. 3B). Gene targeting only with pvINT^{G} vector yielded a very low frequency of *TK* revertants (10^{-7}). In contrast, co-transfection with pvINT^{8OxG} or pvINT^{G} vectors and the I-*Sce*I expression vector pCBASce increased the frequency of *TK* revertants to approximately 10^{-2} (Fig. 4A), indicating that HR-mediated repair of DSB at the I-*Sce*I site enhances targeting efficiency. Interestingly, *TK* revertant frequencies did not differ between cells transfected with pvINT^{8OxG} and pvINT^{G} vectors, indicating that the 8-oxoG adduct in the targeting vector was efficiently delivered to the genome (Fig. 4A). Moreover, in cells transfected with only pCBASce, revertant frequencies were significantly increased from 10^{-4} to 10^{-3} [18–20] (Fig. 4A), indicating that approximately 10% of *TK* revertants in the TATAM system are generated by inter-allelic HR, but not by gene targeting. These revertants were distinguished using the molecular analyses reported below.

TK revertant frequencies were constant until 72 h (Fig. 4B), suggesting that the targeting vector is integrated immediately into the TSCER122 genome. Moreover, *TK* revertant clones increased linearly with quantities of pvINT^{G} targeting vector in the TATAM system (Fig. 4C), indicating that under the present conditions the TATAM system is quantitative and reproducible.

3.3. Determination of mutation frequencies and spectra at integrated 8-oxoG lesions

Table 1 shows mutation frequencies and spectra associated with integration of single 8-oxoG adducts by each targeting vector. The frequencies of pvINT^{G}- (770/888 or 88%) and pvINT^{8OxG}-targeted

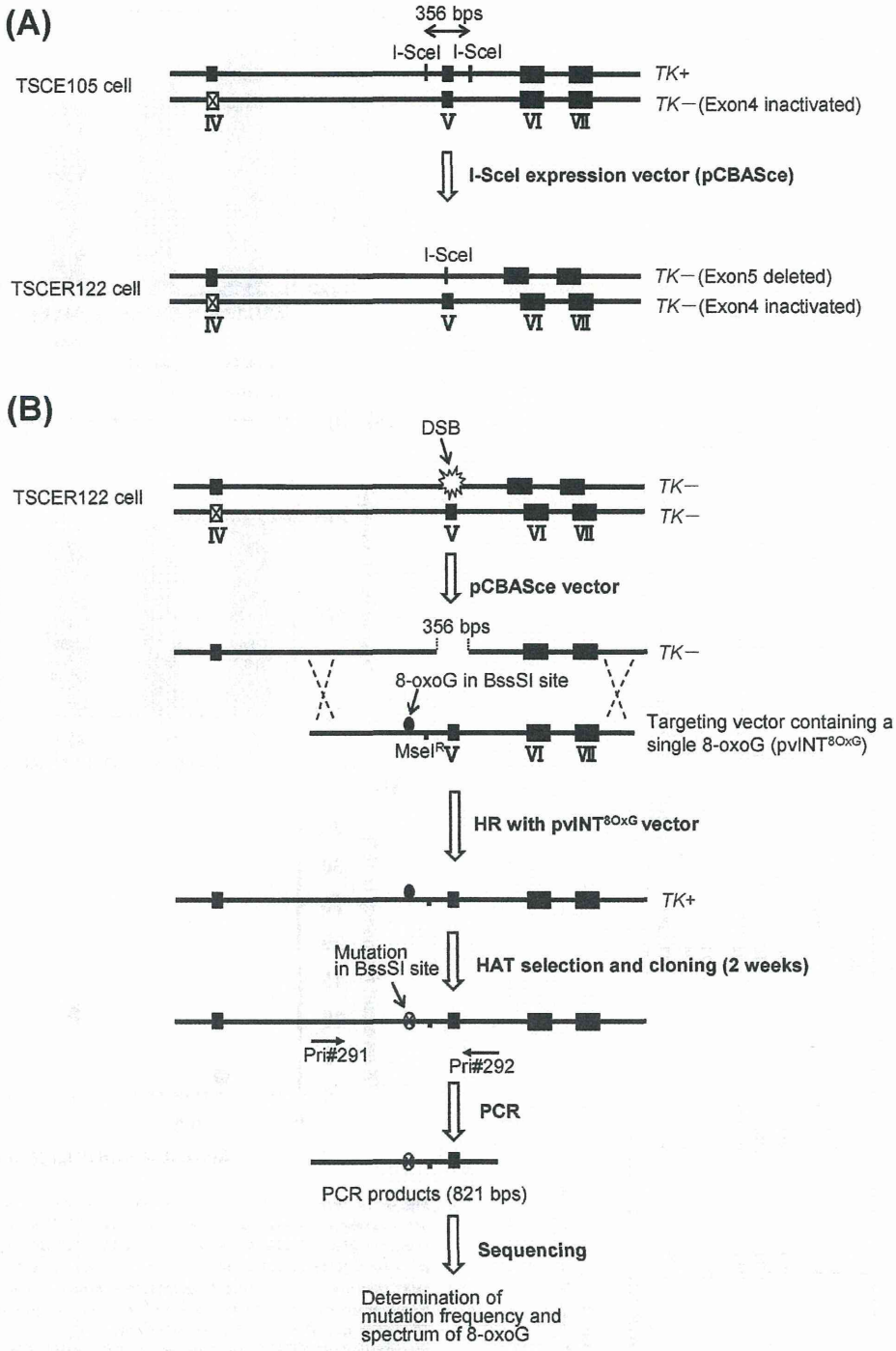

Fig. 3. (A) Development of TSCER122 cells used in the TATAM system. TSCE105 (*TK*+/−) is heterozygous for a point mutation in exon 4 of the *TK* gene and has two I-*Sce*I recognition sites surrounding exon 5 of the *TK*+ allele. Following transfection of the I-*Sce*I expressing vector, DSB occurring at the two I-*Sce*I sites were correctly fused by error-free end-joining and produced a new I-*Sce*I site with a 356-bp deletion containing the entire exon 5, resulting in the *TK*-deficient mutant TSCER122. (B) Principle of the use of HR in the TATAM system. The 8-oxoG-modified targeting vector pvINT^{8OxG} (or pvINT^{G} as a control) and the I-SceI expression plasmid pCBASce were co-transfected into TSCER122 cells. The DSB occurring at the I-*Sce*I site enabled high gene targeting efficiency for the TATAM system by inducing DSB-repair enhanced site-specific HR. The targeting vectors contained *Mse*I^{R} sites, which do not exist in the native *TK* gene and thereby distinguish between targeted and nontargeted revertants. Genomic DNAs were extracted from the clones, and the part of the *TK* gene containing the 8-oxoG-integrated site was amplified by PCR using the primers Pri#291 and #292, as described in Section 2. PCR products were then sequenced using an ABI 3730xl DNA analyzer.

revertants (803/944 or 85%) were similar, and other non-target revertants generated by inter-allelic HR (12% for pvINT^{G} and 15% for pvINT^{8OxG}). These target and non-target revertants were distinguished using *Mse*I enzyme cleavage analyses (Fig. 2B).

Among the sequenced sites generated by integration of 8-oxoG, 86% were repaired or bypassed without causing mutations. Among the remaining 14% of mutations, G:C to T:A transversions were predominant (5.9%), followed by single-base deletions

Table 1
Mutation frequency and spectrum associated with a single integrated 8-oxoG.

Targeting vector	Cell	Experiment	No. of *TK* revertants analyzed	No. of G- or 8-oxoG-integrated revertants	No. of targeted mutants (G or 8-oxoG→X)					Total of point mutation	Others[d]	ND[e]
					X=G	Point mutation			Del.[b]	Ins.[c]			
						T	C	A				
pvINT^{G}	TSCER122	1	250	209	206	0	0	0	0	0	3	0
		2	638	561	551	0	0	0	0	1	9	0
		Total	888	770 (100%)	757 (98%)	0	0	0	0	1 (0.1%)	12	0
pvINT^{8OxG}	TSCER122	1	259	207	176	13	2	1	4	2	5	4
		2	685	596	516	34	8	5	13	4	13	3
		Total	944	803 (100%)	692 (86%)	47 (5.9%)	10 (1.2%)	6 (0.7%)	17 (2.1%)	6 (0.7%)	18	7
pvINT^{8OxG}	TSCER122MYH	1	245	199	171	5	3	1	7	2	7	3
		2	374	308	276	8	5	4	8	1	5	1
		Total	619	507 (100%)	447 (88%)	13 (2.6%)	8 (1.6%)	5 (1%)	15 (2.9%)	3 (0.6%)	12	4

[a] Significantly different from the control value; $P < 0.05$ (Student's *t*-test).
[b] Indicates targeted single-base deletion.
[c] Indicates the sum of targeted C, T, and G insertions.
[d] Non-targeted mutations. See sequence changes shown in Table 2.
[e] Not detectable.

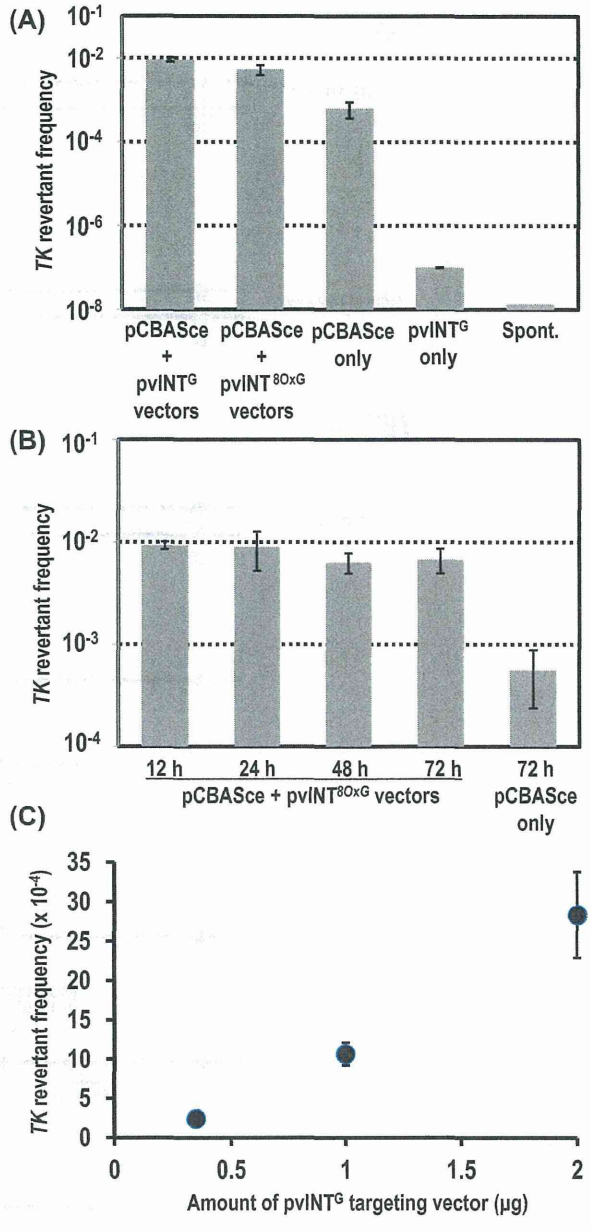

Fig. 4. *TK* revertant frequencies induced by pCBASce and targeting vectors. (A) I-*Sce*I expression vector (pCBASce) and/or pvINT^{8OxG} vector (or pvINT^{G} as a control) were transfected into TSCER122 cells. Three days later, cells were seeded into 96-microwell plates in the presence of HAT to select for *TK*-revertant clones. Two weeks later, microwells containing drug-resistant colonies were counted, and *TK*-revertant frequencies were calculated. (B) No effect of expression period on the frequency of *TK*-revertants; after transfection, cells were cultured for 12, 24, 48, or 72 h, and were then seeded into 96-microwell plates. (C) Dose-dependent relationship between *TK*-revertant frequency and the amount of pvINT^{G} targeting vector; pCBASce (50 μg) and pvINT^{G} (0.4, 1, or 2 μg) vectors were co-transfected into TSCER122 cells and *TK*-revertant frequency increased linearly with increasing quantities of pvINT^{G} targeting vector.

Table 2
Properties of miscellaneous base changes and large deletions at BssSI site.

Other base-changes[a]	pvINT^{G}	pvINT^{8OxG}	
	TSCER122	TSCER122	TSCER122MYH
5′-ctc8tg (original)			
5′-cttgtg	6	1	2
5′-ctcgag	1	1	1
5′-cccgtg	2	2	
5′-ctcgta	1	1	
5′-cttcgtg	2		1
5′-ctctttg		1	2
5′-ccctttg		1	
5′-ctattg		1	
5′-ctcgΔg		1	
5′-ctggtg		2	
5′-ctcgttg		2	
5′-ctcgtcg		1	
5′-ctctgg		1	
5′-ctcttgg			1
5′-cttctg			2
5′-ctcattg			1
5′-ttcttg			1
5′-ctctatg			1
135-bp deletion		1[b]	
6-bp deletion		1[c]	
33-bp deletion		1[d]	
Total	12	18	12

[a] "8" and "Δ" indicate 8-oxoG and single-base deletion, respectively.
[b] 5′-gctgcgcagttgtggatgtacctgtcgtctgctgggggcgtgcgggtggacacagtcccccggcctggggagcctcgtgggagaattaagagttactccgggccaaatggccggagttgtcagatccattacc.
[c] 5′-cctcgt.
[d] 5′-gagcctcgtgggagaattaagagttactccggg.

(2.1%) and G:C to C:G transversions (1.2%). In contrast, control vector integrated lesions did not produce any point mutations. Table 2 shows the miscellaneous base changes observed at low frequency. Base substitutions, single-base deletions and insertions were observed around the 8-oxoG sites. Some of these mutations were also observed in the control experiment (pvINT^{G}). However, three deletional mutations (6, 33, and 135-bp) containing 8-oxoG site observed in cells transfected only with pvINT^{8OxG}.

3.4. Stability of 8-oxoG in pvINT^{8OxG} before targeting integration

DNA repair enzymes such as 8-oxoguanine glycosylase (OGG1) may remove 8-oxoG adducts after transfection of plasmid vectors before integration into the genome [28,32,33]. Thus, assays were performed with competitive 100-bps^{8OxG} and noncompetitive 100-bps^{G} vectors that cannot act as targeting vectors. In these experiments, if the 8-oxoG adduct is efficiently excised from the vectors, the revertant frequency with the competitive vector should be higher than with the non-competitive vector. However, the frequencies of base changes in the *Bss*SI cleavage site, which was not present in the revertants (Fig. 3B), were 18.7 ± 2.0% (26/139) for the noncompetitive vector and 14.3 ± 2.3% (19/132) for the competitive vector. These frequencies did not differ significantly, indicating that 8-oxoG was not efficiently excised from the targeting vector prior to integration into the genome.

3.5. Decreased mutation frequencies of 8-oxoG in TSCER122MYH cells

MYH-overexpressing TSCER122MYH cells were isolated from 5×10^6 TSCER122 cells transfected with *Xmn*I-linearized pCI-MYHβ3 and cultured in 96-microwell plates in the presence of G418, as described in Section 2. MYH expression was 2.1-times higher in TSCER122MYH cells than in wild-type TSCER122 cells (Supplementary Fig. S3). Among the 619 genomic DNAs extracted from TSCER122MYH clones, 507 (82%) were *Mse*I^{R}-bearing clones, indicating that the integration frequency was similar to that of the control (Table 1). The total point mutation frequency (8.7%) decreased a little, but did not differ significantly from that in wild-type TSCER122 cells (10.7%). However, the fraction of G:C to T:A transversions in TSCER122MYH cells (2.6%) was 2.3 times lower than in wild-type cells (5.9%; Table 1).

3.6. 8-oxoG mutations did not differ between NTS and TS of the TK gene

Initially, the TATAM system was devised for NTS of the *TK* gene. Subsequently, we analyzed consequences of 8-oxoG adducts in both NTS and TS of the *TK* gene (Table 3). Introduction of 8-oxoG into the *TK*-TS side of the *Bss*SI site (Supplementary Fig. S1) caused a total point mutation frequency of 10.6%, which was similar to that in the NTS side (10.7%). Mutation spectra were also similar between NTS and TS of the *TK* gene. Interestingly, no single-base deletions were detected in the TS side, whereas the frequency of single-base deletions at the NTS side was 2.1% (Table 3).

4. Discussion

Because the frequency of HR in mammalian cells is generally low, the gene targeting efficiency through HR is $<10^{-6}$ [34,35]. In contrast, gene targeting integration using the present TATAM system (Figs. 1 and 3) was 10^{-3} to 10^{-2} (Fig. 4). This dramatic enhancement of gene targeting efficiency was achieved by site-specific I-*Sce*I, which produces DSB that strongly initiates HR [24,25]. In addition, *TK* revertant frequencies increased linearly with the quantity of targeting vector (Fig. 4C), indicating that gene targeting in the TATAM system is not saturated by the targeting vector under the present conditions, enabling quantitative comparison of the gene targeting efficiencies. Using a new PCR-based method, we prepared high yields (micrograms) of target vectors containing DNA adducts within 5 days. Thus, the TATAM system allows efficient recovery of adduct-integrated clones, and can be used to investigate the genetic consequences of individual adducts at specific sites in the human genome.

Oxidative damage by reactive oxygen species (ROS) occurs frequently in all organisms. Reactions of ROS with DNA produce a large variety of lesions on bases and sugars. Among these, the biological importance of 8-oxoG is widely accepted because of its abundance and mutagenicity [36]. The mutagenicity of 8-oxoG has been well characterized in bacterial and mammalian cells. Specifically, shuttle vectors carrying specific 8-oxoG sites predominantly produce G:C to T:A transversions in *E. coli* and simian kidney cells (COS-7) [15,37]. Kamiya et al. integrated a synthetic c-Ha-ras protooncogene containing 8-hydroxyguanine (8-ohG; hydroxyl form of 8-oxoG) in the second position of codon 12 (GGC) into the murine genome of NIH3T3 cells and demonstrated a preponderance of G:C to T:A transversions among the resulting transformants [38]. In another study, treatments of *Ogg1* deficient *gpt* transgenic mice with the oxidative agent potassium bromate ($KBrO_3$) caused tremendous accumulation of 8-ohG lesions in kidney DNA, which produced a high frequency of mutations in the *gpt* gene [39]. Subsequent mutational spectra analyses revealed that G:C to T:A transversions were the most prevalent, followed by G:C to A:T transitions and small deletions in both wild-type and *Ogg1* deficient *gpt* transgenic mice.

The TATAM system showed that 8-oxoG predominantly caused G:C to T:A transversions followed by single base deletions. These

Table 3
Comparison of mutation specificities of a single 8-oxoG placed in the NTS and TS of inherent *TK* gene.

Targeting vector and location of 8-oxoG[a]	No. of *TK* revertants analyzed	No. of 8-oxoG-integrated revertants	No. of targeted mutants (8-oxoG→X)						Total of point mutation	Others[e]	ND[f]
			X=G	Point mutation			Del.[c]	Ins.[d]			
				T	C	A					
pvINT^{8oxG} 5′ agcctc8tggga 5′ tccgagaggct	944[b]	803 (100%)	692 (86%)	47 (5.9%)	10 (1.2%)	6 (0.7%)	17 (2.1%)	6 (0.7%)	86 (10.7%)	18	7
pvIT^{8oxG} 5′ agcctcgtggga 5′ tccgagcaggct	436	368 (100%)	315 (85%)	29 (7.9%)	8 (2.2%)	1 (0.3%)	0	1 (0.3%)	39 (10.6%)	6	8

[a] "8" indicates 8-oxoG.
[b] Data are taken from Table 1.
[c] Indicates targeted single-base deletions.
[d] Indicates the sum of targeted C, T, and G insertions.
[e] Non-targeted mutations.
[f] Not detectable.

data are consistent with the above reports. However, only 14% of 8-oxoG lesions led to mutations in the system and the remaining 86% of 8-oxoG lesions were restored to G, probably through base excision repair (BER) or TLS (Table 1). Because we did not use drug selection to isolate mutants, the TATAM system enabled both characterization of mutations and evaluation of the efficiency of DNA repair and TLS. To investigate the effects of BER, we constructed TSCER122MYH cells overexpressing the MYH protein, which removes adenine from 8-oxoG:A but not cytosine from 8-oxoG:C [29,40]. Overexpressed MYH only works for 8-oxoG:A that is generated by error-prone TLS. Accordingly, mutation frequencies of G:C to T:A transversions were significantly suppressed in TSCER122MYH cells (2.6%), whereas other mutations occurred with similar frequency, suggesting that MYH in the TATAM system specifically removes adenine from 8-oxoG:A mismatched pairs. These results indicate that the 8-oxoG sites introduced by the TATAM system are processed as those generated by oxidative DNA damage. Use of additional cell types with overexpressed or deficient repair enzymes in the TATAM system will further elucidate DNA repair and TLS mechanisms.

In the present study, the TATAM system characterized mutations induced by xanthine and 8-bromoguanine adducts, which are formed by reactions of ROS and reactive nitrogen species with guanine bases in inflamed tissues [41–43]. As shown in Supplementary Table S1, the predominant mutations (G:C to A:T transitions for xanthine and single-base deletions for 8-bromoguanine) observed in the TATAM system were consistent with previous *in vitro* studies [5,44–46]. Thus, the TATAM system accurately characterizes mutation spectra of various endogenous DNA adducts in the human genome.

In this study, we investigated mutational properties of 8-oxoG on TS and NTS of the *TK* gene using the TATAM system. It is widely accepted that transcription-coupled repair (TCR) is initiated upon irreversible stalling of RNA polymerase II on TS of bulky pyrimidine dimers [47–49]. However, the mechanisms of transcriptional arrest at site-specific 8-oxoG adducts remain unknown. Although pauses and partial blockage by the lesions has been demonstrated using purified RNA polymerase II *in vitro* [50,51], other studies show efficient bypass of 8-oxoG lesions using cell extracts and luciferase reporter assays [52–54]. Pastoriza-Gallego et al. showed that transcriptional arrest by 8-oxoG can vary with proximal promoter strengths and nucleotide sequences [54]. As shown in Table 3, the mutational properties of 8-oxoG on NTS and TS were almost the same, indicating that no preferential strand repair of 8-oxoG adducts in the *TK* gene, and implying that the TCR pathway is not initiated by such lesions.

Interestingly, single-base deletions were detected on NTS, but not on TS in the *TK* gene, potentially reflecting the sequence context of neighboring 8-oxoG rather than the TCR pathway. In a previous study of mammalian cells, oligonucleotides containing 8-oxoG in shuttle vector systems predominantly produced G:C to T:A transversions, whereas other frequently detected mutations were influenced by neighboring sequences and no single base deletions were observed [55]. Thus, the mechanisms behind 8-oxoG-associated single-base deletions in the present TATAM experiments remain unclear. In *in vitro* DNA synthesis experiments using synthetic templates, single-base deletions were generated depending on the neighboring sequences and the polymerase used (mammalian DNA polymerase α, β, and γ, and *E. coli* Klenow fragment pol I or pol III) [56–58]. In contrast, single-base deletions, particularly of guanine, were infrequently observed in transgenic gene mutation assays after treatment of animals with $KBrO_3$ [59]. The TATAM system detects unique mutations caused by 8-oxoG (Table 2, 3). Because some mutations were also produced by the control targeting vector pvINT^{G}, artifactual effects of gene targeting may cause occasional gene mutations. However, some mutations,

particularly large deletions (6–135 bp), were only specifically generated by the pvINT^{8OxG} vector (Table 3), implying an association with DSB. In the BER pathway, 8-oxoG is excised by DNA glycosylase and creates an abasic site, which is incised by AP endonucleases and generates single strand breaks. Repair of these lesions can lead to DSB through collapsed replication forks during cell cycle progression [60]. Hence introduction of DNA adducts into introns of the *TK* gene using the TATAM system enables rescue from various genetic consequences of DNA adducts, such as large deletions, offering a significant advantage for investigations of mutation spectra, and evading selection biases.

In conclusion, the TATAM system we developed here can be used to introduce any synthetic DNA adduct into specific regions of the human genome, providing a valuable tool for quantitative investigations of the fate of individual adducts in the human genome. Moreover, this method can be used to determine the biological characteristics and phenomena of DNA adducts in human cells overexpressing or deficient in specific enzymes, such as DNA polymerases and DNA repair proteins.

Conflict of interest

The authors declare that there are no conflicts of interest.

Acknowledgements

We acknowledge several helpful discussions with Dr. Takehiko Nohmi and Dr. Katsuyoshi Horibata (National Institute of Health Sciences). This work was supported by the Grant-in-Aid for Scientific Research (B) from the Ministry of Education, Culture, Sports, Science and Technology and for Health Science Foundation (H24-food-general-011) from the Ministry of Health, Welfare and Labor in Japan.

Appendix A. Supplementary data

Supplementary data associated with this article can be found, in the online version, at http://dx.doi.org/10.1016/j.dnarep.2014.01.003.

References

[1] T. Lindahl, Instability and decay of the primary structure of DNA, Nature 362 (1993) 709–715.
[2] T.A. Kunkel, The high cost of living, in: American Association for Cancer Research Special Conference: Endogenous Sources of Mutations, Fort Myers, FL, USA, 11–15 November 1998, Trends in Genetics: TIG 15 (1999) 93–94.
[3] P.H. Chou, S. Kageyama, S. Matsuda, K. Kanemoto, Y. Sasada, M. Oka, K. Shinmura, H. Mori, K. Kawai, H. Kasai, H. Sugimura, T. Matsuda, Detection of lipid peroxidation-induced DNA adducts caused by 4-oxo-2(E)-nonenal and 4-oxo-2(E)-hexenal in human autopsy tissues, Chemical Research in Toxicology 23 (2010) 1442–1448.
[4] R.A. Kanaly, S. Matsui, T. Hanaoka, T. Matsuda, Application of the adductome approach to assess intertissue DNA damage variations in human lung and esophagus, Mutation Research 625 (2007) 83–93.
[5] A. Sassa, T. Ohta, T. Nohmi, M. Honma, M. Yasui, Mutational specificities of brominated DNA adducts catalyzed by human DNA polymerases, Journal of Molecular Biology 406 (2011) 679–686.
[6] R.D. Wood, DNA repair in eukaryotes, Annual Review of Biochemistry 65 (1996) 135–167.
[7] C. Masutani, R. Kusumoto, A. Yamada, N. Dohmae, M. Yokoi, M. Yuasa, M. Araki, S. Iwai, K. Takio, F. Hanaoka, The XPV (xeroderma pigmentosum variant) gene encodes human DNA polymerase eta, Nature 399 (1999) 700–704.
[8] D.R. Spitz, E.I. Azzam, J.J. Li, D. Gius, Metabolic oxidation/reduction reactions and cellular responses to ionizing radiation: a unifying concept in stress response biology, Cancer Metastasis Reviews 23 (2004) 311–322.
[9] J.C. Delaney, J.M. Essigmann, Biological properties of single chemical-DNA adducts: a twenty year perspective, Chemical Research in Toxicology 21 (2008) 232–252.
[10] J.M. Essigmann, C.L. Green, R.G. Croy, K.W. Fowler, G.H. Buchi, G.N. Wogan, Interactions of aflatoxin B1 and alkylating agents with DNA: structural and functional studies, Cold Spring Harbor Symposia on Quantitative Biology 47 (Pt 1) (1983) 327–337.
[11] N. Shrivastav, D. Li, J.M. Essigmann, Chemical biology of mutagenesis and DNA repair: cellular responses to DNA alkylation, Carcinogenesis 31 (2010) 59–70.
[12] A.K. Basu, J.M. Essigmann, Site-specifically modified oligodeoxynucleotides as probes for the structural and biological effects of DNA-damaging agents, Chemical Research in Toxicology 1 (1988) 1–18.
[13] E.L. Loechler, C.L. Green, J.M. Essigmann, In vivo mutagenesis by O^6-methylguanine built into a unique site in a viral genome, Proceedings of the National Academy of Sciences of the United States of America 81 (1984) 6271–6275.
[14] A.K. Basu, E.L. Loechler, S.A. Leadon, J.M. Essigmann, Genetic effects of thymine glycol: site-specific mutagenesis and molecular modeling studies, Proceedings of the National Academy of Sciences of the United States of America 86 (1989) 7677–7681.
[15] M. Moriya, Single-stranded shuttle phagemid for mutagenesis studies in mammalian cells: 8-oxoguanine in DNA induces targeted G.C→T.A. transversions in simian kidney cells, Proceedings of the National Academy of Sciences of the United States of America 90 (1993) 1122–1126.
[16] H. Nishida, M. Kawanishi, T. Takamura-Enya, T. Yagi, Mutagenic specificity of N-acetoxy-3-aminobenzanthrone, a major metabolically activated form of 3-nitrobenzanthrone, in shuttle vector plasmids propagated in human cells, Mutation Research 654 (2008) 82–87.
[17] K.C. Cheng, D.S. Cahill, H. Kasai, S. Nishimura, L.A. Loeb, 8-Hydroxyguanine, an abundant form of oxidative DNA damage, causes G–T and A–C substitutions, Journal of Biological Chemistry 267 (1992) 166–172.
[18] K.S. Ellison, E. Dogliotti, T.D. Connors, A.K. Basu, J.M. Essigmann, Site-specific mutagenesis by O^6-alkylguanines located in the chromosomes of mammalian cells: influence of the mammalian O^6-alkylguanine-DNA alkyltransferase, Proceedings of the National Academy of Sciences of the United States of America 86 (1989) 8620–8624.
[19] K.B. Altshuler, C.S. Hodes, J.M. Essigmann, Intrachromosomal probes for mutagenesis by alkylated DNA bases replicated in mammalian cells: a comparison of the mutagenicities of O^4-methylthymine and O^6-methylguanine in cells with different DNA repair backgrounds, Chemical Research in Toxicology 9 (1996) 980–987.
[20] L. Izhar, O. Ziv, I.S. Cohen, N.E. Geacintov, Z. Livneh, Genomic assay reveals tolerance of DNA damage by both translesion DNA synthesis and homology-dependent repair in mammalian cells, Proceedings of the National Academy of Sciences of the United States of America 110 (2013) E1462–E1469.
[21] M. Honma, M. Izumi, M. Sakuraba, S. Tadokoro, H. Sakamoto, W. Wang, F. Yatagai, M. Hayashi, Deletion, rearrangement, and gene conversion; genetic consequences of chromosomal double-strand breaks in human cells, Environmental and Molecular Mutagenesis 42 (2003) 288–298.
[22] M. Honma, M. Sakuraba, T. Koizumi, Y. Takashima, H. Sakamoto, M. Hayashi, Non-homologous end-joining for repairing I-SceI-induced DNA double strand breaks in human cells, DNA Repair (Amsterdam) 6 (2007) 781–788.
[23] Y. Takashima, M. Sakuraba, T. Koizumi, H. Sakamoto, M. Hayashi, M. Honma, Dependence of DNA double strand break repair pathways on cell cycle phase in human lymphoblastoid cells, Environmental and Molecular Mutagenesis 50 (2009) 815–822.
[24] P. Rouet, F. Smih, M. Jasin, Expression of a site-specific endonuclease stimulates homologous recombination in mammalian cells, Proceedings of the National Academy of Sciences of the United States of America 91 (1994) 6064–6068.
[25] M. Porteus, Homologous recombination-based gene therapy for the primary immunodeficiencies, Annals of the New York Academy of Sciences 1246 (2011) 131–140.
[26] A.J. Grosovsky, B.N. Walter, C.R. Giver, DNA-sequence specificity of mutations at the human thymidine kinase locus, Mutation Research 289 (1993) 231–243.
[27] K. Maasho, A. Marusina, N.M. Reynolds, J.E. Coligan, F. Borrego, Efficient gene transfer into the human natural killer cell line, NKL, using the Amaxa nucleofection system, Journal of Immunological Methods 284 (2004) 133–140.
[28] T. Ohtsubo, K. Nishioka, Y. Imaiso, S. Iwai, H. Shimokawa, H. Oda, T. Fujiwara, Y. Nakabeppu, Identification of human MutY homolog (hMYH) as a repair enzyme for 2-hydroxyadenine in DNA and detection of multiple forms of hMYH located in nuclei and mitochondria, Nucleic Acids Research 28 (2000) 1355–1364.
[29] M. Takao, Q.M. Zhang, S. Yonei, A. Yasui, Differential subcellular localization of human MutY homolog (hMYH) and the functional activity of adenine:8-oxoguanine DNA glycosylase, Nucleic Acids Research 27 (1999) 3638–3644.
[30] T. Arakawa, T. Ohta, Y. Abiko, M. Okayama, I. Mizoguchi, T. Takuma, A polymerase chain reaction-based method for constructing a linear vector with site-specific DNA methylation, Analytical Biochemistry 416 (2011) 211–217.
[31] E.E. Furth, W.G. Thilly, B.W. Penman, H.L. Liber, W.M. Rand, Quantitative assay for mutation in diploid human lymphoblasts using microtiter plates, Analytical Biochemistry 110 (1981) 1–8.
[32] K. Nishioka, T. Ohtsubo, H. Oda, T. Fujiwara, D. Kang, K. Sugimachi, Y. Nakabeppu, Expression and differential intracellular localization of two major forms of human 8-oxoguanine DNA glycosylase encoded by alternatively spliced OGG1 mRNAs, Molecular Biology of the Cell 10 (1999) 1637–1652.
[33] H. Ide, M. Kotera, Human DNA glycosylases involved in the repair of oxidatively damaged DNA, Biological and Pharmaceutical Bulletin 27 (2004) 480–485.
[34] K.M. Vasquez, K. Marburger, Z. Intody, J.H. Wilson, Manipulating the mammalian genome by homologous recombination, Proceedings of the National Academy of Sciences of the United States of America 98 (2001) 8403–8410.
[35] S. So, Y. Nomura, N. Adachi, Y. Kobayashi, T. Hori, Y. Kurihara, H. Koyama, Enhanced gene targeting efficiency by siRNA that silences the expression of the Bloom syndrome gene in human cells, Genes to Cells 11 (2006) 363–371.

[36] B. van Loon, E. Markkanen, U. Hubscher, Oxygen as a friend and enemy: how to combat the mutational potential of 8-oxo-guanine, DNA Repair (Amsterdam) 9 (2010) 604–616.
[37] X. Tan, A.P. Grollman, S. Shibutani, Comparison of the mutagenic properties of 8-oxo-7,8-dihydro-2′-deoxyadenosine and 8-oxo-7,8-dihydro-2′-deoxyguanosine DNA lesions in mammalian cells, Carcinogenesis 20 (1999) 2287–2292.
[38] H. Kamiya, K. Miura, H. Ishikawa, H. Inoue, S. Nishimura, E. Ohtsuka, c-Ha-ras containing 8-hydroxyguanine at codon 12 induces point mutations at the modified and adjacent positions, Cancer Research 52 (1992) 3483–3485.
[39] T. Arai, V.P. Kelly, O. Minowa, T. Noda, S. Nishimura, High accumulation of oxidative DNA damage, 8-hydroxyguanine, in Mmh/Ogg1 deficient mice by chronic oxidative stress, Carcinogenesis 23 (2002) 2005–2010.
[40] J.P. McGoldrick, Y.C. Yeh, M. Solomon, J.M. Essigmann, A.L. Lu, Characterization of a mammalian homolog of the *Escherichia coli* MutY mismatch repair protein, Molecular and Cellular Biology 15 (1995) 989–996.
[41] T. Nguyen, D. Brunson, C.L. Crespi, B.W. Penman, J.S. Wishnok, S.R. Tannenbaum, DNA damage and mutation in human cells exposed to nitric oxide in vitro, Proceedings of the National Academy of Sciences of the United States of America 89 (1992) 3030–3034.
[42] J.P. Henderson, J. Byun, M.V. Williams, M.L. McCormick, W.C. Parks, L.A. Ridnour, J.W. Heinecke, Bromination of deoxycytidine by eosinophil peroxidase: a mechanism for mutagenesis by oxidative damage of nucleotide precursors, Proceedings of the National Academy of Sciences of the United States of America 98 (2001) 1631–1636.
[43] T. Asahi, H. Kondo, M. Masuda, H. Nishino, Y. Aratani, Y. Naito, T. Yoshikawa, S. Hisaka, Y. Kato, T. Osawa, Chemical and immunochemical detection of 8-halogenated deoxyguanosines at early stage inflammation, Journal of Biological Chemistry 285 (2010) 9282–9291.
[44] R. Eritja, D.M. Horowitz, P.A. Walker, J.P. Ziehler-Martin, M.S. Boosalis, M.F. Goodman, K. Itakura, B.E. Kaplan, Synthesis and properties of oligonucleotides containing 2′-deoxynebularine and 2′-deoxyxanthosine, Nucleic Acids Research 14 (1986) 8135–8153.
[45] H. Kamiya, T. Sakaguchi, N. Murata, M. Fujimuro, H. Miura, H. Ishikawa, M. Shimizu, H. Inoue, S. Nishimura, A. Matsukage, et al., In vitro replication study of modified bases in ras sequences, Chemical and Pharmaceutical Bulletin 40 (1992) 2792–2795.
[46] M. Yasui, N. Suzuki, H. Miller, T. Matsuda, S. Matsui, S. Shibutani, Translesion synthesis past 2′-deoxyxanthosine, a nitric oxide-derived DNA adduct, by mammalian DNA polymerases, Journal of Molecular Biology 344 (2004) 665–674.
[47] V.A. Bohr, C.A. Smith, D.S. Okumoto, P.C. Hanawalt, DNA repair in an active gene: removal of pyrimidine dimers from the DHFR gene of CHO cells is much more efficient than in the genome overall, Cell 40 (1985) 359–369.
[48] B.A. Donahue, S. Yin, J.S. Taylor, D. Reines, P.C. Hanawalt, Transcript cleavage by RNA polymerase II arrested by a cyclobutane pyrimidine dimer in the DNA template, Proceedings of the National Academy of Sciences of the United States of America 91 (1994) 8502–8506.
[49] P.C. Hanawalt, G. Spivak, Transcription-coupled DNA repair: two decades of progress and surprises, Nature Reviews Molecular Cell Biology 9 (2008) 958–970.
[50] I. Kuraoka, M. Endou, Y. Yamaguchi, T. Wada, H. Handa, K. Tanaka, Effects of endogenous DNA base lesions on transcription elongation by mammalian RNA polymerase II. Implications for transcription-coupled DNA repair and transcriptional mutagenesis, Journal of Biological Chemistry 278 (2003) 7294–7299.
[51] N. Charlet-Berguerand, S. Feuerhahn, S.E. Kong, H. Ziserman, J.W. Conaway, R. Conaway, J.M. Egly, RNA polymerase II bypass of oxidative DNA damage is regulated by transcription elongation factors, EMBO Journal 25 (2006) 5481–5491.
[52] S. Tornaletti, L.S. Maeda, R.D. Kolodner, P.C. Hanawalt, Effect of 8-oxoguanine on transcription elongation by T7 RNA polymerase and mammalian RNA polymerase II, DNA Repair (Amsterdam) 3 (2004) 483–494.
[53] E. Larsen, K. Kwon, F. Coin, J.M. Egly, A. Klungland, Transcription activities at 8-oxoG lesions in DNA, DNA Repair (Amsterdam) 3 (2004) 1457–1468.
[54] M. Pastoriza-Gallego, J. Armier, A. Sarasin, Transcription through 8-oxoguanine in DNA repair-proficient and Csb(−)/Ogg1(−) DNA repair-deficient mouse embryonic fibroblasts is dependent upon promoter strength and sequence context, Mutagenesis 22 (2007) 343–351.
[55] H. Kamiya, Mutagenic potentials of damaged nucleic acids produced by reactive oxygen/nitrogen species: approaches using synthetic oligonucleotides and nucleotides: survey and summary, Nucleic Acids Research 31 (2003) 517–531.
[56] L.B. Bloom, X. Chen, D.K. Fygenson, J. Turner, M. O'Donnell, M.F. Goodman, Fidelity of *Escherichia coli* DNA polymerase III holoenzyme. The effects of beta, gamma complex processivity proteins and epsilon proofreading exonuclease on nucleotide misincorporation efficiencies, Journal of Biological Chemistry 272 (1997) 27919–27930.
[57] T.A. Kunkel, Frameshift mutagenesis by eucaryotic DNA polymerases in vitro, Journal of Biological Chemistry 261 (1986) 13581–13587.
[58] S. Shibutani, A.P. Grollman, On the mechanism of frameshift (deletion) mutagenesis in vitro, Journal of Biological Chemistry 268 (1993) 11703–11710.
[59] T. Yamaguchi, M. Wei, N. Hagihara, M. Omori, H. Wanibuchi, S. Fukushima, Lack of mutagenic and toxic effects of low dose potassium bromate on kidneys in the Big Blue rat, Mutation Research 652 (2008) 1–11.
[60] J.L. Parsons, G.L. Dianov, Co-ordination of base excision repair and genome stability, DNA Repair (Amsterdam) 12 (2013) 326–333.

DNA Repair 15 (2014) 21–28

Contents lists available at ScienceDirect

DNA Repair

journal homepage: www.elsevier.com/locate/dnarepair

In vivo evidence that phenylalanine 171 acts as a molecular brake for translesion DNA synthesis across benzo[*a*]pyrene DNA adducts by human DNA polymerase κ

Akira Sassa[a,b,1], Tetsuya Suzuki[a,2], Yuki Kanemaru[a,3], Naoko Niimi[a,4], Hirofumi Fujimoto[c], Atsushi Katafuchi[a,5], Petr Grúz[a], Manabu Yasui[a], Ramesh C. Gupta[d], Francis Johnson[d], Toshihiro Ohta[b], Masamitsu Honma[a], Noritaka Adachi[e], Takehiko Nohmi[a,*]

[a] *Division of Genetics and Mutagenesis, National Institute of Health Sciences, 1-18-1 Kamiyoga, Setagaya-ku, Tokyo 158-8501, Japan*
[b] *School of Life Sciences, Tokyo University of Pharmacy and Life Sciences, Hachioji-shi, Tokyo 192-0392, Japan*
[c] *Division of Radiological Protection and Biology, National Institute of Infectious Diseases, 1-23-1 Toyama, Shinjuku-ku, Tokyo 162-8640, Japan*
[d] *Department of Pharmacological Sciences and Department of Chemistry, Stony Brook University, Stony Brook, NY 11794-3400, USA*
[e] *Graduate School of Nanobioscience, Yokohama City University, 22-2 Seto, Kanazawa-ku, Yokohama 236-0027, Japan*

ARTICLE INFO

Article history:
Received 6 October 2013
Received in revised form
10 December 2013
Accepted 29 December 2013
Available online 21 January 2014

Keywords:
Translesion DNA synthesis
DNA polymerase κ
Benzo[*a*]pyrene diolepoxide-N^2-guanine

ABSTRACT

Humans possess multiple specialized DNA polymerases that continue DNA replication beyond a variety of DNA lesions. DNA polymerase kappa (Pol κ) bypasses benzo[*a*]pyrene diolepoxide-N^2-deoxyguanine (BPDE-N^2-dG) DNA adducts in an almost error-free manner. In the previous work, we changed the amino acids close to the adducts in the active site and examined the bypass efficiency. The substitution of alanine for phenylalanine 171 (F171A) enhanced by 18-fold *in vitro*, the efficiencies of dCMP incorporation opposite (−)- and (+)-*trans-anti*-BPDE-N^2-dG. In the present study, we established human cell lines that express wild-type Pol κ (*POLK*+/−), F171A (*POLK* F171A/−) or lack expression of Pol κ (*POLK*−/−) to examine the *in vivo* significance. These cell lines were generated with Nalm-6, a human pre-B acute lymphoblastic leukemia cell line, which has high efficiency for gene targeting. Mutations were analyzed with shuttle vectors having (−)- or (+)-*trans-anti*-BPDE-N^2-dG in the *supF* gene. The frequencies of mutations were in the order of *POLK*−/− > *POLK*+/− > *POLK* F171A/− both in (−)- and (+)-*trans-anti*-BPDE-N^2-dG. These results suggest that F171 may function as a molecular brake for bypass across BPDE-N^2-dG by Pol κ and raise the possibility that the cognate substrates for Pol κ are not BP adducts in DNA but may be lesions in DNA induced by endogenous mutagens.

1. Introduction

The human genome is continuously exposed to a variety of endogenous and exogenous genotoxic agents, which induce DNA damage. These DNA lesions strongly block DNA replication mediated by replicative DNA polymerases (Pols), thereby inducing cell toxicity. Cells have evolved various defense mechanisms against genotoxic agents such as antioxidants, detoxication enzymes, DNA repair and so on. Translesion DNA synthesis (TLS) is one of defense mechanisms to overcome the toxic effects of DNA lesions [1,2]. In fact, human cells possess more than 10 specialized Pols, which can take over the primer DNA from the replicative Pols and continue primer extension beyond the template lesion, i.e., TLS [3–5]. After the successful TLS, the specialized Pols transfer the continued primer DNA to the replicative Pols, what make the chromosome replication complete and rescue the damaged cells [6]. TLS can also suppress mutations by incorporation of correct dNMPs opposite

* Corresponding author. Present address: Biological Safety Research Center, National Institute of Health Sciences, Tokyo 158-8501, Japan. Tel.: +81 3 3700 1564; fax: +81 3 3700 1622.
E-mail address: nohmi@nihs.go.jp (T. Nohmi).
[1] Present address: Laboratory of Structural Biology, NIEHS, 111 T.W. Alexander Drive, Research Triangle Park, NC 27709, USA.
[2] Present address: Division of Health Effects Research, National Institute of Occupational Safety and Health, Kanagawa 214-8585, Japan.
[3] Present address: Division of Toxicology, Department of Pharmacology, Toxicology and Therapeutics, Showa University School of Pharmacy, Tokyo 142-8555, Japan.
[4] Present address: Department of Sensory and Motor Systems, Tokyo Metropolitan Institute of Medical Science, 2-1-6 Kamikitazawa, Setagaya-ku, Tokyo 156-8506, Japan.
[5] Present address: Department of Radiation Life Sciences, Fukushima Medical University, Fukushima 960-1295, Japan.

1568-7864/$ – see front matter © 2014 Elsevier B.V. All rights reserved.
http://dx.doi.org/10.1016/j.dnarep.2013.12.008

the damaged base in the template. A typical example of such error-free TLS is the correct insertion of dAMP opposite thymine dimer induced by ultraviolet light (UV) by human Pol η [7,8]. Defects in the *XPV* gene encoding Pol η are molecular basis for the human genetic disease Xeroderma pigmentosum variant, the sufferers of which are highly susceptible to UV-induced skin cancer. In general, the specialized Pols are less accurate for DNA replication compared to the replicative Pols [9,10]. Therefore, some of TLS mediated by the specialized Pols are error prone and generate sequence changes, i.e., incorrect dNMPs incorporation opposite the damaged template base, thereby causing base substitutions [11,12]. Thus, TLS can be a double-edged sword, as the mechanisms contributing to genetic integrity can themselves result in mutations.

Human Pol κ is one of the specialized Pols and belongs to the Y family, the most predominant Pol family for TLS [6,13–15]. Unlike other Y-family members, i.e., Pol η, Pol ι and REV1, the orthologs of Pol κ present in bacteria, Eukarya and Archaea [16–18]. Other Y-family Pols are present only in Eukarya. Although Pol κ is suggested to be involved in TLS across a number of DNA lesions, i.e., N^2-guanyl adducts induced by polycyclic aromatic hydrocarbons and alkylating agents, a C8-guanyl adduct generated by 2-amino-1-methyl-6-phenylimidazo[4,5-*b*]pyridine (PhIP), the thymine glycol lesion, 8-oxo-guanine and interstrand DNA crosslinks [19–29], the best characterized one is N^2-guanyl adducts induced by benzo[*a*]pyrene (BP). BP is an environmental mutagen that is present in cigarette smoke and released to the air as a combustion product of fossil fuel [30]. Upon contact with lung tissue, BP is metabolized to various reactive intermediates, the most mutagenic and carcinogenic of which is benzo[*a*]pyrene-7,8-dihydrodiol-9,10-epoxide (BPDE) [30,31]. Pol κ appears to be involved in error-free TLS across N^2-guanyl adducts induced by BPDE, i.e., (−)- and (+)-*trans-anti*-BPDE-N^2-dG (hereafter, we call them (−)-BPDE-dG and (+)-BPDE-dG) [19,23,25,32]. Pol κ strongly binds to DNA containing (−)-BPDE-dG, and preferentially incorporates dCMP opposite both (−) and (+) lesions [25]. Several lines of evidence with cultured mammalian cells suggest that Pol κ is involved in error-free TLS across BPDE DNA adducts *in vivo* [24,33,34]. However, the catalytic mechanism underlying the error-free TLS across the lesions is not fully understood yet.

To understand better the catalytic mechanism, we have replaced amino acids proximal to the adducts with alanine and examined the TLS activities of the purified enzymes *in vitro* [35]. The amino acids that were replaced were phenylalanine 171 (F171), arginine 175 (R175) and leucine 197 (L197), based on the ternary complex of Pol κ with DNA and an incoming nucleotide [36]. R175 to alanine (R175A) and L197 to alanine (L197A) exhibited either no or a slight decrease in their effects on the TLS activities. Unexpectedly, however, the substitution of F171 to alanine (F171A) increased the TLS activities by about 20 fold and significantly enhanced the binding ability to DNA containing (−)-BPDE-dG. In the present study, we established human cells that express the F171A variant Pol κ and examined the sensitivity to (−)- and (+)-BPDE-dG in DNA. Such cells exhibited significantly lower mutation frequencies induced by the adducts compared to the cells expressing wild-type Pol κ. From the current *in vivo* studies along with our previous *in vitro* results, we conclude that F171 acts as a molecular brake for Pol κ-mediated TLS across (−)- and (+)-BDPE-dG in DNA. A possible mechanism by which F171 inhibits TLS across BPDE adducts in DNA and possible cognate substrates for Pol κ are discussed.

2. Materials and methods

2.1. Cell culture and DNA transfection

The human pre-B cell line Nalm-6 and its derivatives were cultured in RPMI 1640 (Nacalai Tesque) with 10% calf serum (Thermo Fisher Scientific) and 50 μM 2-mercaptoethanol at 37 °C in an atmosphere of 5% CO_2 and 100% humidity. DNA transfection for gene targeting was performed as previously described [37]. Briefly, the linearized targeting construct DNA (2 μg) was transfected into 2.0×10^6 cells that were suspended in 0.1 mL of KitT solution with supplement 1 by using the Nucleofector I according to the manufacturer's instructions (Lonza). After cultivation for 24–48 h, the cells were re-plated at a density of $\sim 10^6$ per 90-mm dish at agarose medium containing 400 μg/ml hygromycin B (Wako) or 0.5 μg/ml puromycin (Wako). Alternatively, the appropriate numbers of cells were plated into 96-well plates in medium containing one or other of the same medium. After 2–3 weeks incubation, the resulting drug resistant colonies were isolated and cultured for stock frozen permanents for preparation of cell extracts, total RNA and genomic DNA.

2.2. Targeting constructs for POLK knock-out or POLK F171A knock-in cells

The targeting vectors were constructed by using the simple vector construction method based on the Multi Site Gateway® Technology (Life Technologies) as described [38]. For knock-out of *POLK*, genomic fragments were obtained by PCR amplification with Ex Taq Pol (Takara Bio) from Nalm-6 genomic DNA using primers KO-5armF (5′-GGGGACAACTTTGTATAGAAAAGTTGTGCTGTCTAAGAGACTGATAAT-3′) and KO-5armR (5′-GGGGACTGCTTTTTTGTACAAACTTGTAGCTACCTACTATATCTAGTTATAA-3′) for the 5′-arm, and KO-3armF (5′-GGGGACAGCTTTCTTGTACAAAGTGGTGACACAGAAGGGTTTGCTCAC-3′) and KO-3armR (5′-GGGGACAACTTTGTATAATAAAGTTGCAGGGTGGTCTCAAACTCCTG-3′) for the 3′-arm. The targeting vector was linearized with *Ahd*I and transfected into the Nalm-6 cells as described above. The targeted clones were confirmed by the Southern blotting analysis. For knock-in of *POLK F171A*, genomic fragments were obtained from Nalm-6 genomic DNA by PCR with KOD-FX (Toyobo) using primers KI-5armF (5′-GGGGACAACTTTGTATAGAAAAGTTGATGGTCTTGGTAACTTCCCTATGTTGC-3′) and KI-5armR (5′-GGGGACTGCTTTTTTGTACAAACTTGTGAGCCATCGCCATCGCACTC-3′) for the 5′-arm, and KI-3armF (5′-GGGGACAGCTTTCTTGTACAAAGTGGACCTTGCTCTACCTGGAGTTGGC-3′) and KI-3′armR (5′-GGGGACAACTTTGTATAATAAAGTTGTGCTCCCCTCTCCTCCACCAC-3′) for the 3′-arm. The mutation of TTT to GCT at codon 171, which directed an amino acid substitution of F171 to alanine, was introduced into the 3′-arm by PCR-mediated site-directed mutagenesis. The targeting vector was linearized with *Pme*I and transfected into $POLK^{+/-(Hygr)}$ cells. The targeting clones were confirmed by the genomic PCR using primers 5′-GAAGAGGTTCACTAGTACTGGCCATTGC-3′ and 5′-GCCAGAAGTTTTGCTGAGTTAAAGTACGACT-3′. Insertion of the puromycin-resistance gene (Pur^r) into the *POLK* wild-type allele in $POLK^{F171A/-(Hygr)}$ cell was confirmed by RT-PCR followed by sequencing analysis as described below and the genomic PCR using primers 5′-GATAATAATGGTTTCTTAGACGTCGCGC-3′ and 5′-GAAGAGGTTCACTAGTACTGGCCATTGC-3′, which amplifies ~5 kb fragment when both $Puro^r$ and the hygromycin-resistance gene (Hyg^r) are targeted into the same *POLK* allele and no fragments are generated when $Puro^r$ and Hyg^r are targeted into the discrete *POLK* allele. The $Puro^r$ and the Hyg^r were removed by introduction of Cre recombinase expression vector by Nucleofector I.

2.3. Southern blot analysis

Southern blotting was performed as previously described [39]. Briefly, 10 μg of genomic DNA was digested with *Eco*RV, then subjected to electrophoresis in 0.8% agarose gel and the DNA was transferred onto a hybond-N^+ membrane (GE Healthcare Bio-Sciences),

followed by Southern hybridization with a ^{32}P-labeled probe that was obtained by PCR amplification from Nalm-6 genomic DNA using the following primers: 5′-CATCATGAGGACCCTGAACTATC-3′ and 5′-TCAGGT AGTCCACGAGCTTCG-3′.

2.4. Western blot analysis

Total cell extracts were prepared from exponentially growing cells and subjected to electrophoresis in 10% SDS-polyacrylamide gel and then electro-transferred onto a PVDF membrane (Millipore). The membrane was soaked with blocking buffer including 5% skim milk, then incubated with either polyclonal antibody against Pol κ or mouse anti-β-actin monoclonal antibody (Sigma–Aldrich), and finally incubated with peroxidase-conjugated anti-rabbit immunoglobulin or anti-mouse IgG conjugated to horseradish peroxidase (GE Healthcare Bio-Sciences). The polyclonal antibody was prepared by TaKaRa (Shiga, Japan) by immunization of a rabbit with purified C-terminally truncated 10 × HisTag human Pol κ $_{1\text{-}559}$ [25]. The proteins were visualized by chemiluminescence using the ECL system (GE Healthcare Bio-Sciences).

2.5. RNA extraction and RT-PCR

Total RNA was extracted using RNeasy kit (Qiagen). For RT-PCR, total RNA was transcribed into cDNA using SuperScript III First-Strand Synthesis System (Invitrogen). The synthesized cDNA was used as the template for PCR using Ex Taq Pol (Takara Bio) with gene-specific primers 5′-GATAATAAAGCAGGGATGG-3′ and 5′-GCACTAGCTGTCAGTGTTGT-3′. The sequence of the *POLK*$^{F171A/-}$ cells were analyzed with 3130 Avant genetic analyzer (Applied Biosystems).

2.6. Construction of closed circular double-stranded plasmid DNA containing a single (−)- or (+)-BPDE-dG

The nucleotide position 123 of the *supF* gene was chosen for the (−)-BPDE-dG or (+)-BPDE-dG incorporation site because it has been recognized as a BPDE-induced mutational hotspot for G:C to T:A transversions [40]. The 21-mer oligodeoxynucleotide bearing BPDE-dG (5′-GCGGCCAAAGXGAGCAGACTC-3′, where X represent (−)-BPDE-dG or (+)-BPDE-dG) was synthesized as previously reported [41]. The pMY189 single-stranded DNA was prepared in *Escherichia coli* (*E. coli*) JM109 strain using VCSM13 helper phage as previously described [42]. The 5′-phosphorylated unmodified, (−)-BPDE-dG or (+)-BPDE-dG-modified oligodeoxynucleotide was annealed with pMY189 single-stranded DNA, and closed circular double-stranded DNA containing a single dG:dC, (−)-BPDE-dG:dC, or (+)-BPDE-dG:dC pair was synthesized and purified as previously described [43].

2.7. SupF forward mutation assay and sequencing analysis

Plasmid pMY189 with or without (−)-BPDE-dG or (+)-BPDE-dG (1 μg) was transfected into 2.0×10^6 cells by using Nucleofector I as described above. After 72 h of culturing in medium, propagated plasmids were extracted from the cells by the method described by Stary and Sarasin [44]. The recovered DNA was treated with *Dpn*I to digest unreplicated plasmids. The recovered plasmids were introduced into the KS40/pOF105 indicator bacteria [45] with a MicroPulser Electroporator (Bio-Rad Laboratories). To select *E. coli* with a mutated *supF* gene, the transformed cells were plated onto Luria-Bertani (LB) agar plates containing nalidixic acid (50 μg/ml), streptomycin (100 μg/ml), ampicillin (150 μg/ml), chloramphenicol (30 μg/ml), 5-bromo-4-chloro-3-indolyl-β-D-galactopyranoside (80 μg/ml), and isopropyl-β-D-thiogalactopyranoside (23.8 μg/ml). To determine the total number of transformants, the transformed cells were plated onto LB plates containing ampicillin (150 μg/ml) and chloramphenicol (30 μg/ml). The nucleotide sequences of the *supF* gene were analyzed by DNA sequencing, as previously described [46].

2.8. Statistical analysis

The statistical significance was examined using the Student's *t* test. Levels of $P < 0.05$ were considered significant.

3. Results

3.1. Establishment of *POLK*$^{+/-}$ and *POLK*$^{-/-}$ cells

POLK resides on chromosome 5 (coordinates 74.8–74.9 Mb of the human genome presented in Ensembl) and includes 15 exons. To disrupt the *POLK* gene in the human pre-B lymphoblastic leukemia cell line, Nalm-6, a targeting vector was constructed to delete exon 6 of the *POLK* gene, resulting in a frameshift (Fig. 1A). The targeting vectors have Hyg^r for the first targeting or Puro^r for the second targeting flanked by the *loxP* site and also contain the diphtherotoxin A (DT-A) gene to exclude random integrants. As a result of the first targeting, we obtained one heterozygous disrupted clone (*POLK*$^{+/-(Hygr)}$) out of 132 hygromycin-resistant clones. For the second targeting, the puromycin-resistance targeting vectors were transfected into the *POLK*$^{+/-(Hygr)}$ clone. We obtained one homo-disrupted clone (*POLK*$^{-(Puror)/-(Hygr)}$) out of 158 puromycin-resistant clones from *POLK*$^{+/-(Hygr)}$. The targeted disruption into the *POLK* gene was verified by Southern blot analysis using the *Eco*RV-digested genomic DNA with an external 3′ probe (Fig. 2A). To remove the Hyg^r and Puro^r cassettes from the resulting clones, the Cre expression vector was electroporated into the clones obtained above. The expression of the protein was then examined by Western blot analysis with anti-Pol κ antibody (Fig. 2B), which indicated that Pol κ protein was expressed in *POLK*$^{+/+}$ and *POLK*$^{+/-}$ cells, but not in *POLK*$^{-/-}$ cell. Loss of the expression of *POLK* mRNA in *POLK*$^{-/-}$ was confirmed by RT-PCR analysis (Fig. 2C). The doubling time of the *POLK*$^{+/-}$ (20.8 ± 0.59 h) or *POLK*$^{-/-}$ (20.9 ± 0.91 h) cell was similar to that of *POLK*$^{+/+}$ (20.2 ± 0.95 h) cell, showing that the knock-out of *POLK* does not significantly influence the proliferation rate of Nalm-6 cell line.

3.2. Establishment of *POLK*$^{F171A/-}$ cell

The knock-in cell that expresses *POLK* F171A (*POLK*$^{F171A/-}$) was generated from *POLK*$^{+/-(Hygr)}$ cells that possess a Hyg^r cassette in the *POLK* knock-out allele. The targeting vector was constructed to introduce the mutation (TTT to GCT) into exon 5 (Fig. 1B), resulting in the substitution of phenylalanine for alanine at codon 171. The targeting vector has a Puro^r cassette flanked by the *loxP* site and contains the DT-A gene. The targeting vector was linearized with *Pme*I and electroporated into the *POLK*$^{+/-(Hygr)}$ cell. After selecting the cells with puromycin, we obtained 7 positive clones, in which the Puro^r cassette was introduced into the targeted locus of *POLK* wild type or *POLK* knock-out allele, out of 133 puromycin-resistant clones. We further examined the expression of *POLK* mRNA and confirmed the sequence of the cDNA in clones (Fig. 2D). We obtained 2 clones that expressed the mutant *POLK* mRNA, i.e., *POLK* F171A, out of 7 clones, suggesting that the expected mutation was introduced into *POLK* wild-type allele in these clones. We also confirmed that the Puro^r cassette was introduced into the targeted locus of *POLK* wild type allele, but not *POLK* knock-out allele in these clones by genomic PCR (data not shown). The equivalent construct without the mutation was used to generate the mock-treated cell (*POLK*$^{mock/-}$). Puro^r and Hyg^r cassettes